

ADAS601: Differential emission measure analysis

Given a set of observed spectral intensities, $G(T_e)$ functions and elemental abundances, the program evaluates an estimate for the emission measure differential in temperature, using the integral inversion algorithm of A. M. Thompson. Selection of the input data files for elemental abundances, $G(T_e)$ functions, and observed spectral intensities can be made at any time during the analysis. The output consists of displays of the differential emission measure vs. electron temperature and the reconstructed observed spectral intensity ratios. A tabulation of these quantities is also produced. The input set of $G(T_e)$ functions can be displayed and examined at any time.

Background theory:

In order to derive the emission measure differential in temperature, we require to solve the integral equation

$$I_{u \rightarrow l} = \frac{1}{4\pi} \mathcal{A}(Z) \int_0^{\infty} G_{u \rightarrow l}(T_e) \phi(T_e) dT_e \quad 7.1.1$$

for a set of, say, m spectral lines. In 7.1.1, $I_{u \rightarrow l}$ is the intensity of a spectral line from a column of optically thin plasma due to a transition from upper level u to lower level l , $\mathcal{A}(Z) \equiv N_{tot}/N_H$ is the fractional elemental abundance assumed to be known, Z the element's nuclear charge, $\phi(T_e)$ the emission measure differential in temperature, as defined in the ADAS506 section.

Note that in equation 7.1.1 the dependence on the electron density has been dropped, which would have lead to the formulation of the bi-variate integral inversion problem. G and ϕ would then have been functions of electron temperature and electron density, and the integral over both variables. The simplified formulation expressed by equation 7.1.1 is achieved by selecting only those spectral lines whose G -functions have a slow dependence on electron density, at least in the physical range of interest. Resonance lines have such properties in most cases. However, in order to achieve the best approximation for the G -functions, the slow dependence on the electron density is taken into account by assuming an approximate constant pressure or constant density for the plasma. This is equivalent to selecting an approximate dependence $N_e = N_e(T_e)$, so that the G -functions can be considered effectively dependent on T_e only. G -functions stored as ADF20 are computed for a grid of constant electron pressure for this purpose.

Equation 7.1.1 is solved by the *data adaptive smoothing approach* of A. M. Thompson. The integral is discretised (product integration method) as

$$\begin{aligned} I_{u \rightarrow l} &= \frac{1}{4\pi} \mathcal{A}(Z) \int_0^{\infty} G_{u \rightarrow l}(T_e) \phi(T_e) dT_e \\ &= \frac{1}{4\pi} \mathcal{A}(Z) \sum_{i=1}^N \int_{T_{j-1}}^{T_j} G_{u \rightarrow l}(T_e) \phi(T_e) dT_e \\ &= \frac{1}{4\pi} \mathcal{A}(Z) \sum_{j=1}^N \phi_j^* \int_{T_{j-1}}^{T_j} G_{u \rightarrow l}(T_e) \phi_0(T_e) dT_e \end{aligned} \quad 7.1.2$$

where

$$\phi_j^* \equiv \frac{\int_{T_{j-1}}^{T_j} G_{u \rightarrow l}(T_e) \phi(T_e) dT_e}{\int_{T_{j-1}}^{T_j} G_{u \rightarrow l}(T_e) \phi_0(T_e) dT_e} \quad 7.1.3$$

represents a weighted average of $\phi(T_e)/\phi_0(T_e)$ between T_{j-1} and T_j . $\phi_0(T_e)$ is an initial estimate of $\phi(T_e)$ towards which we shall smooth the solution. This process can be viewed as scaling the solution using an expected gross behaviour of $\phi(T_e)$ as represented by $\phi_0(T_e)$. The advantage is to reduce the dynamic range of the problem before the actual regularised solution (see below) is obtained. This has been proven to prevent uneven smoothing, with the solution being over-smoothed at large values of ϕ and under-smoothed at low values, when the source function (the differential emission measure) span a large dynamic range.

The prior function $\phi_0(T_e)$ is evaluated as follows. $G_{u \rightarrow l}(T_e)$ is approximated by $\bar{G}_{u \rightarrow l} \delta(T_e - T_{u \rightarrow l}^{\max})$, where

$$\bar{G}_{u \rightarrow l} \equiv \int_0^{\infty} G_{u \rightarrow l}(T_e) dT_e \quad 7.1.4$$

$T_{u \rightarrow l}^{\max}$ being the temperature corresponding to the maximum of $G_{u \rightarrow l}(T_e)$ and δ the Dirac's delta function. A crude estimate of ϕ is then

$$\bar{\phi}(T_{u \rightarrow l}^{\max}) = \frac{4\pi}{\mathcal{A}(Z)} \frac{I_{u \rightarrow l}}{\bar{G}_{u \rightarrow l}} \quad 7.1.5$$

A cubic B-spline is now fitted to the values $\log(\bar{\phi}(T_{u \rightarrow l}^{\max}))$ to obtain a smooth representation for $\phi_0(T_e)$. This representation can only yields features comparable to the typical kernel in width (estimated, to this purpose, to be $\approx 1/2$ decade). The knot points of the B-spline representation are therefore selected approximately $\approx 1/2$ decade apart. In other words, we obtain

$$\log(\phi_0(T_e)) \equiv S(\log(T_e)) \quad 7.1.6$$

where $S(\log(T_e))$ denotes the B-spline representation with interior knots about $\approx 1/2$ decade apart.

The B-spline fit described above provides a satisfactory estimate of $\phi_0(T_e)$ between the maximum and minimum values of $T_{u \rightarrow l}^{\max}$. It is necessary, however, to extrapolate $\phi_0(T_e)$ beyond these boundaries. This is done as follows.

For

$$T > \max[T_{u \rightarrow l}^{\max}] \quad \text{and} \quad [d\phi_0/dT_e]_{\max[T_{u \rightarrow l}^{\max}]} < 0$$

or

$$T < \min[T_{u \rightarrow l}^{\max}] \quad \text{and} \quad [d\phi_0/dT_e]_{\min[T_{u \rightarrow l}^{\max}]} > 0 \quad ,$$

$\log(\phi_0(T_e))$ is extrapolated linearly. This allows the value of $\phi_0(T_e)$ to decrease smoothly while ensuring that it is always positive.

For

$$T > \max[T_{u \rightarrow l}^{\max}] \quad \text{and} \quad [d\phi_0/dT_e]_{\max[T_{u \rightarrow l}^{\max}]} < 0$$

or

$$T < \min[T_{u \rightarrow l}^{\max}] \quad \text{and} \quad [d\phi_0/dT_e]_{\min[T_{u \rightarrow l}^{\max}]} < 0 ,$$

$\phi_0(T_e)$ is extrapolated linearly. This is done because any rapid power law variation in $\phi_0(T_e)$ beyond the maximum and minimum of $T_{u \rightarrow l}^{\max}$ is likely to lead a gross inconsistency between the values of $\overline{\phi}(T_{u \rightarrow l}^{\max})$ and the corresponding averaged value of $\phi_0(T_e)$.

Equation 7.1.1 is then written as

$$g_i = \sum_{j=1}^N H_{ij} f_j + \varepsilon_i \quad (i = 1, 2, \dots, m) \quad 7.1.7$$

which is the canonical form for inverse problems. In 7.1.7, $f_j \equiv \phi_j^*$ is the quantity to be estimated at the *recovery points* T_j ($j = 1, 2, \dots, N$), $g_i \equiv I_{u \rightarrow l}/s_i$ is the data, $\varepsilon_i * s_i$ is the data noise so that ε_i can be regarded as a Gaussian error of constant variance and s_i a weighting parameter or an estimate of the noise variance on the i th spectral line, and

$$H_{ij} \equiv \frac{\Delta(Z)}{4\pi} \frac{1}{s_i} \int_{T_{j-1}}^{T_j} G_i(T_e) \phi_0(T_e) dT_e \quad . \quad 7.1.8$$

Equation 7.1.7 is solved by a regularisation approach. In the method of regularisation the extra information required to stabilise the inversion is introduced by a smoothness condition on the source function. A solution is obtained by solving the optimisation problem

$$\min_{\lambda} \left\{ \sum_{i=1}^m \left(g_i - \sum_{j=1}^N H_{ij} \hat{f} \right)^2 + \lambda \Phi(\hat{f}) \right\} \quad 7.1.9$$

where λ is a smoothing parameter representing the weight attached to the smoothing constraint $\Phi(\hat{f})$ (a linear functional of f), and \hat{f} is the estimate of f . The functional $\Phi(\hat{f})$ represents a prior information about the function f . A choice for this functional derives from the minimisation of the norm of the second derivative of the solution. In other words, of all the solutions that can fit the data the one is chosen that minimises

$$\|\Phi \hat{f}\|_2^2 = \|\hat{f}''\|_2^2 = \int |\hat{f}''(y)|^2 dy \quad 7.1.10$$

This choice of the linear functional defines the second order regularisation problem and is the one adopted for the solution of equation 7.1.7.

Representing the second derivative by second - order differences, 7.1.9 can be written as

$$\min_{\lambda} \left\{ \sum_{i=1}^m \left(g_i - \sum_{j=1}^N H_{ij} \hat{f} \right)^2 + \lambda \left(\sum_{j=1}^N \hat{f}_{j+1} - 2\hat{f}_j + \hat{f}_{j-2} \right)^2 \right\} \quad 7.1.11$$

with an appropriate re-scaling of the regularisation parameter. In order to avoid explicit end conditioning, $\hat{f}_0 = \hat{f}_{N+1} = 0$.

Equation 7.1.9 or 7.1.11 can be expressed in matrix form as

$$(\mathbf{H}^T \mathbf{H} + \lambda \Phi) \hat{\mathbf{f}} = \mathbf{H}^T \mathbf{g} \quad 7.1.12$$

The smoothing parameter λ is selected according to

$$\min_{\lambda} \frac{\|\mathbf{H}\hat{\mathbf{f}} - \mathbf{g}\|^2}{(\text{trace}[\mathbf{H}^T \mathbf{H} + \lambda \mathbf{C}])^2} \quad 7.1.13$$

where \mathbf{C} is the Hessian matrix of $\Phi(\hat{f})$. This method has the attractive property that we do not need to know explicitly the value of the noise variance of the data point but only their ratio. That is if the true standard deviation of the noise on the i -th element is $\sigma_i = \sigma_0 s_i$ then the scaling factor σ_0 can be calculated *a posteriori* using

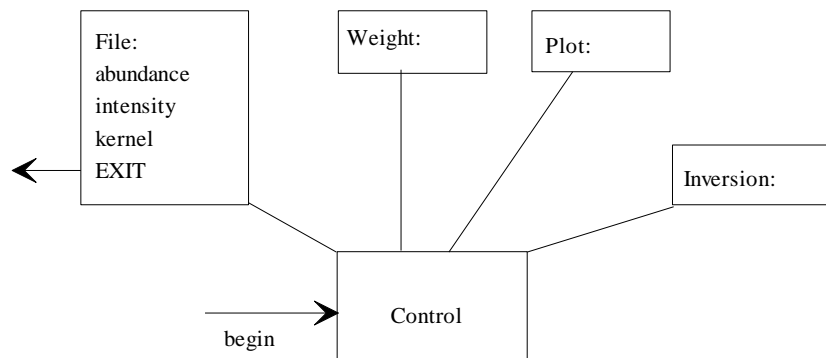
$$\sigma_0^2 = \frac{\|\mathbf{H}\hat{\mathbf{f}} - \mathbf{g}\|^2}{(\text{trace}[\mathbf{H}^T \mathbf{H} + \lambda \mathbf{C}])} \quad 7.1.14$$

The implementation of this procedure and practical application to solar observations performed by the SERTS-89 rocket are described in [1]. Given a DEM curve this method can evaluate the elemental abundances, as illustrated in [2]. It may be helpful to cite these sources in addition to the ADAS manual.

Program steps:

These are summarised in figure 7.1.

Figure 7.1



Interactive parameter comments:

The organisation of the interactive windows differs in ADAS601 from the ADAS norm. Initiate ADAS601 from the ADAS6 series menu. The 'control window' is displayed first.

The **Control window** has the appearance shown below:

1. There are various actions activated by clicking on the names at a). Each yield a drop down menu for further sub-selection. Information on the actions taken is shown in the various display sub-windows at b), c) and d). There are three input data file name information windows, the temperature information window at c), the smoothing information window and then at the bottom of the control window, shorter information windows for the weighting strategy and the current activity. One can jump freely between actions, but on the first use of this program, the 'File' action must be taken first and files loaded sequentially (see below).

The **File** action drops down the menu shown at a) below:

2. Clicking on the file type opens the usual form of ADAS file selection window shown below.

3. The data type sought is shown at a)
4. The central ADAS database has no formal data collections of the three types required here, but only sample data. It is suggested that you use the same organisation and main sub-directory naming as the ADAS example. Clicking the *Central data* or *User*

data buttons sets up a Data root of the ADAS pattern automatically. Personal data for the program ADAS601 should be held in the sub-directory

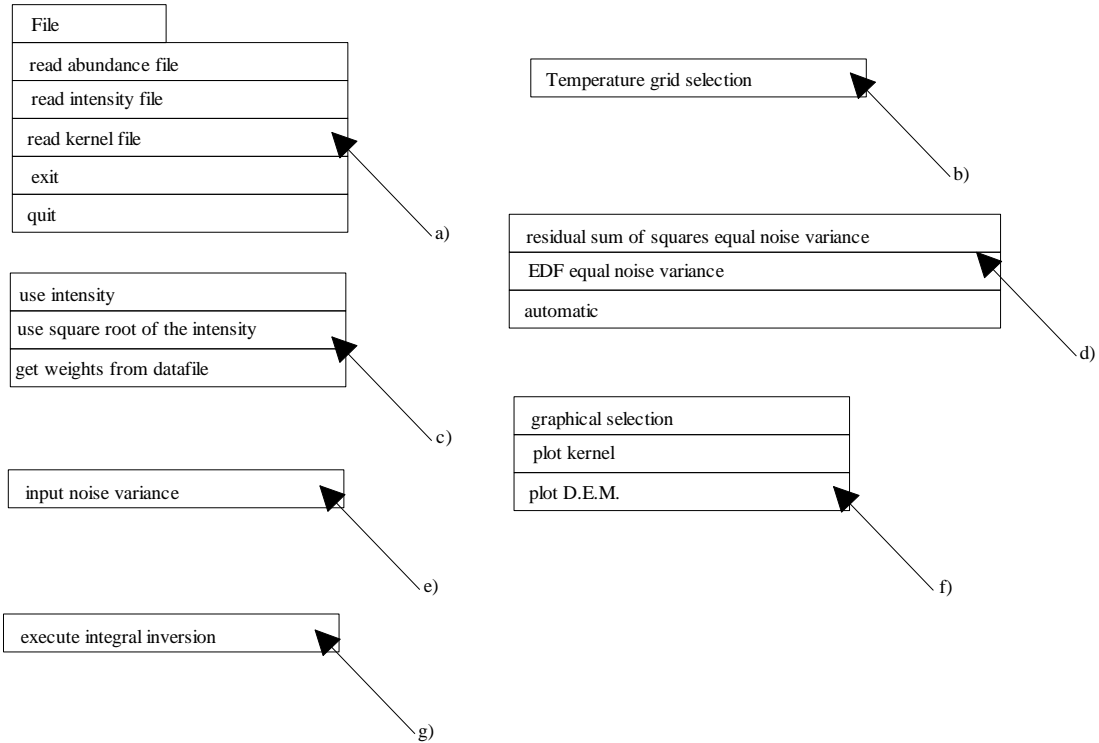
././<user>/adas/arch601

corresponding to the ADAS central sub-directory

././adas/adas/arch601.

Further sub-directories of /arch601 should be assigned, namely, /abundance , /intensity and /kernel. Thus your abundance files should be held in the sub-directory

././<user>/adas/arch601/abundance/...



5. It is convenient to set up an additional sub-directory */run* to hold output data from the program. Move to this sub-directory before initiating ADAS if you wish to ensure output files are placed directly into this sub-directory.
6. All three files must be identified before executing the integral inversion.
7. The intensity file has the standard format shown below:

	Spectr. wavelength	configuration	configuration	bI nd	G-in
C + 3	312.429	2s1(2)0(0.5) -	3p1(2)1(0.5)	1	5
C + 3	312.4	2s1(2)0(0.5) -	3p1(2)1(1.5)	1	6
C + 3	384.032	2p1(2)1(0.5) -	3d1(2)2(1.5)	2	7
C + 3	384.2	2p1(2)1(1.5) -	3d1(2)2(1.5)	2	8
C + 3	384.165	2p1(2)1(1.5) -	3d1(2)2(1.5)	0	9
C IV	419.718	2p1(2)1(1.5) -	3s1(2)0(0.5)	0	-4

(contd.)

```

=====
observed      observed      uncert.
wavelength    intensity
|-----|-----|-----|-----|
312.429       14.2          7.2
312.429
384.032       8.6           3.3
384.65        9.5           2.5
419.718       12.4          2.5
=====

```

8. The observed intensity can be given either in *ergs cm⁻² s⁻¹*, as in the example above, or in *photons cm⁻² s⁻¹*. The program will recognise the units from the magnitude. Units can be mixed in the same input data file.
9. The abundance file is of the simple structure shown below:

O	2.470E-04
NE	3.530E-05
SI	3.920E-05
MG	4.470E-05
S	8.630E-06
FE	3.920E-05
CA	2.940E-06

10. Abundances can be given either as a fraction $N(Z)/N_H$, as in the example above, or in log scale with $\log(N_H)=12.0$. In this latter case, '*H 12.0*' must appear in the data (see the abundance file example *../abund.anders_grevesse*).
11. The kernel file is of the form produced directly as the collection file from ADAS506. Note that you must keep to precisely the same formatting conventions for your personal files of these types.

The **Temperature** action drops down the menu shown at b) above. When you click on this, the temperature sub-window at c) in the control window is reproduced with the boxes editable. Note that entry of any one of the fields causes consistent modification of the others.

The **Weight** action drops down the menu shown at c) above. Click your choice for weighting of the observed intensities. The last choice from the data file uses the variance estimate of the intensity measurement usually provided as part of the observed intensity data (see the structure of an intensity file). This is the default if no selection is made.

The **Smoothing** action drops down the menu shown at d) above

The **Noise** action drops down the menu shown at e) above.

The **Plot** action drops down the menu shown at f) above. Clicking the graphical selection button pops up the standard ADAS output options window below:

ADAS601 OUTPUT OPTIONS

Graphical Output

Graph Title

Explicit Scaling

X-min :
X-max :

Y-min :
Y-max :

Enable Hard Copy Replace

File name :

Default Device

Text Output Replace

File name :

12. Click the plot kernel button to show a simple graph of the $G(\text{Te})$ functions available in the kernel file.
13. A valid DEM plot is available once the integral inversion has been performed once.

The **Run** action drops down the menu shown at g) above.

14. Click on the execute integral inversion button to initiate the integral inversion calculation.
15. After completion of at least one calculation the differential emission measure becomes available for plotting as above.

Illustration:

Figure 7.1a shows a plot of kernel data, that is the set of $G(\text{Te})$ functions contained in the selected kernel file. Figure 7.1b show the resulting differential emission measure for the demonstration case in ADAS. Table 7.1a shows the standard text output from the code.

Figure 7.1a

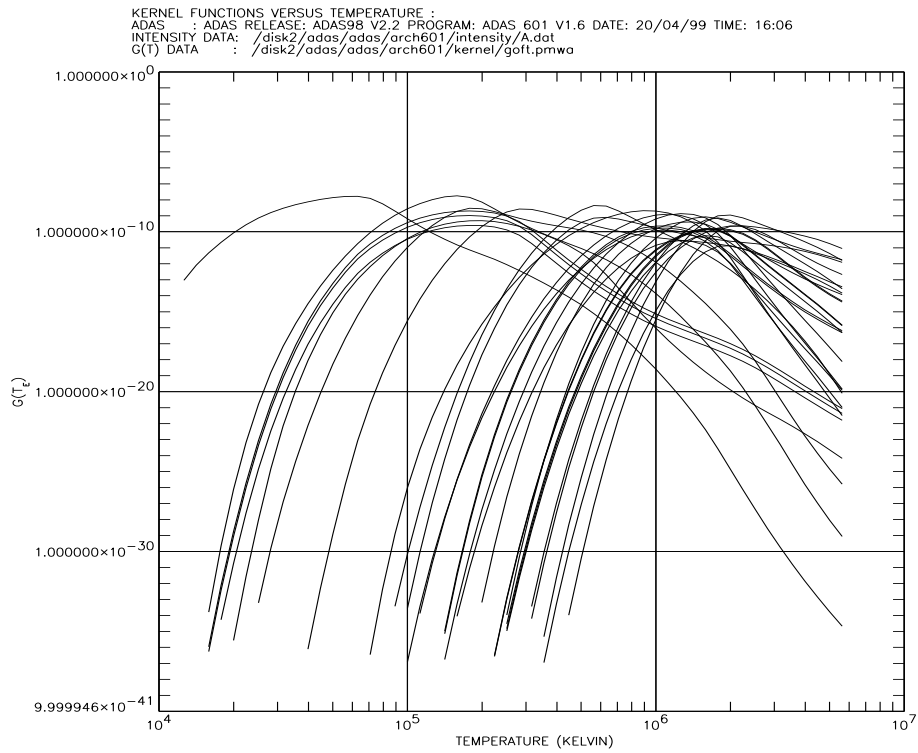


Figure 7.1b

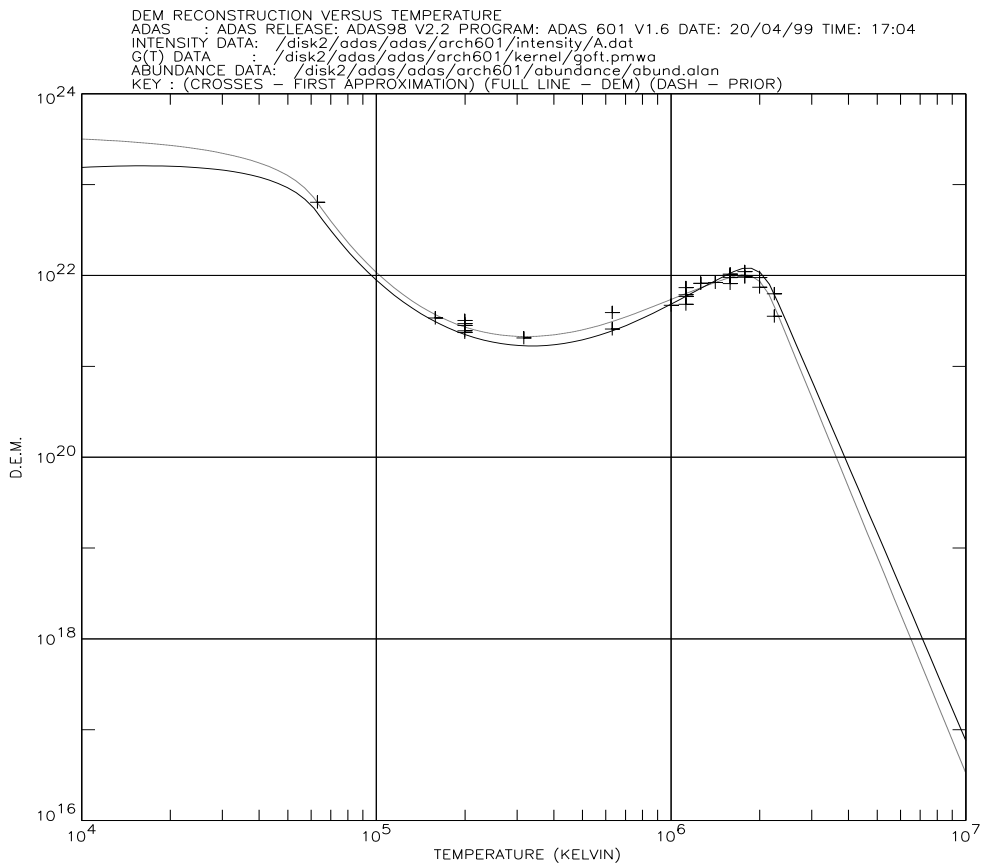


Table 7.1a

ADAS RELEASE: ADAS98 V2.2 PROGRAM: ADAS 601 V1.6 DATE: 20/04/99 TIME: 17:06
 ***** TABULAR OUTPUT FROM INTEGRAL INVERSION - PROGRAM: ADAS 601 V1.6 - DATE: 20/04/99 *****

INTENSITY DATA FILE NAME: /disk2/adas/adas/arch601/intensity/A.dat
 KERNEL DATA FILE NAME: /disk2/adas/adas/arch601/kernel/goft.pmwa
 ABUNDANCE DATA FILE NAME: /disk2/adas/adas/arch601/abundance/abund.alan

CONSTANT VARIANCE = 0.011398431
 SMOOTHING PARAMETER = 6592.4239

----- SINGLE LINES -----										
ION	SPECTROSCOPIC WAVELENGTH	RECONSTRUCTED INTENSITY			Sum[H(i,*)]	OBSERVED INTENSITY		WEIGHT	(Ir-Io)^2/Var	QFR
		ph/cm2/s	erg/cm2/s			ph/cm2/s	erg/cm2/s			
O + 3	608.4000	1.809e+12	5.907e+01	1.142e+13	1.835e+12	5.991e+01	1.959e+11	1.754e-02	9.859e-01	
O + 3	787.7100	7.888e+12	1.989e+02	4.978e+13	8.539e+12	2.153e+02	9.117e+11	5.092e-01	9.238e-01	
O + 3	790.2000	1.541e+13	3.873e+02	9.721e+13	1.538e+13	3.866e+02	1.642e+12	2.421e-04	1.002e+00	
O + 5	1031.9100	2.231e+13	4.295e+02	1.368e+14	2.075e+13	3.994e+02	2.215e+12	4.958e-01	1.075e+00	
NE+ 5	469.8300	5.261e+11	2.224e+01	3.337e+12	5.024e+11	2.124e+01	5.364e+10	1.946e-01	1.047e+00	
NE+ 7	780.3200	3.716e+12	9.459e+01	2.091e+13	3.933e+12	1.001e+02	4.199e+11	2.677e-01	9.448e-01	
SI+ 2	1206.5100	1.261e+14	2.076e+03	8.962e+14	1.242e+14	2.045e+03	1.326e+13	1.991e-02	1.015e+00	
SI+ 8	342.9900	2.135e+12	1.236e+02	1.120e+13	2.513e+12	1.455e+02	2.683e+11	1.989e+00	8.494e-01	
SI+ 8	349.9100	2.915e+12	1.655e+02	1.530e+13	2.741e+12	1.556e+02	2.926e+11	3.532e-01	1.063e+00	
SI+ 9	347.4300	7.513e+12	4.296e+02	3.620e+13	7.636e+12	4.366e+02	8.152e+11	2.260e-02	9.839e-01	
SI+10	303.5800	1.919e+13	1.255e+03	8.607e+13	1.777e+13	1.163e+03	1.897e+12	5.564e-01	1.080e+00	
S + 4	786.4800	3.424e+12	8.647e+01	2.149e+13	3.361e+12	8.489e+01	3.588e+11	3.050e-02	1.019e+00	
S + 5	933.3800	5.460e+11	1.162e+01	3.470e+12	5.937e+11	1.264e+01	6.339e+10	5.674e-01	9.196e-01	
S +10	281.4000	8.319e+11	5.873e+01	3.648e+12	1.032e+12	7.285e+01	1.102e+11	3.298e+00	8.061e-01	
S +10	285.8400	9.644e+11	6.702e+01	4.229e+12	1.044e+12	7.255e+01	1.115e+11	5.106e-01	9.237e-01	
S +11	288.4500	1.146e+12	7.892e+01	4.752e+12	1.051e+12	7.238e+01	1.122e+11	7.168e-01	1.090e+00	
CA+ 8	466.2300	6.194e+11	2.639e+01	3.962e+12	6.429e+11	2.739e+01	6.864e+10	1.172e-01	9.634e-01	
FE+ 8	171.0700	1.809e+13	2.101e+03	1.015e+14	1.764e+13	2.048e+03	1.883e+12	5.830e-02	1.026e+00	
FE+ 9	345.7200	1.481e+12	8.510e+01	7.806e+12	1.463e+12	8.406e+01	1.562e+11	1.328e-02	1.012e+00	
FE+ 9	174.5300	1.488e+13	1.693e+03	7.788e+13	1.128e+13	1.284e+03	1.204e+12	8.926e+00	1.319e+00	
FE+10	352.2500	4.247e+11	2.395e+01	2.109e+12	4.552e+11	2.567e+01	4.860e+10	3.948e-01	9.329e-01	
FE+ 5	180.4100	2.092e+13	2.304e+03	1.035e+14	2.221e+13	2.446e+03	2.371e+12	2.945e-01	9.421e-01	
FE+12	348.1800	3.201e+12	1.826e+02	1.441e+13	3.144e+12	1.794e+02	3.357e+11	2.872e-02	1.018e+00	
FE+12	359.6400	1.127e+12	6.226e+01	5.075e+12	1.179e+12	6.512e+01	1.259e+11	1.693e-01	9.561e-01	
FE+12	241.3800	2.763e+12	2.273e+02	1.243e+13	2.963e+12	2.438e+02	3.163e+11	4.015e-01	9.324e-01	
FE+13	211.3100	1.492e+13	1.402e+03	6.453e+13	1.530e+13	1.438e+03	1.633e+12	5.441e-02	9.751e-01	
FE+14	417.2600	2.878e+11	1.370e+01	1.203e+12	2.798e+11	1.332e+01	2.987e+10	7.088e-02	1.028e+00	
FE+14	284.1600	2.337e+13	1.634e+03	9.745e+13	2.992e+13	2.092e+03	3.194e+12	4.204e+00	7.811e-01	
FE+15	360.7400	4.529e+12	2.494e+02	1.818e+13	4.218e+12	2.323e+02	4.503e+11	4.760e-01	1.074e+00	

----- BLENDS -----											
ION	SPECTROSCOPIC WAVELENGTH	RECONSTRUCTED INTENSITY			Sum[H(i,*)]	OBSERVED INTENSITY		WEIGHT	(Ir-Io)^2/Var	QFR	Iblnd
		ph/cm2/s	erg/cm2/s			ph/cm2/s	erg/cm2/s				

CHISQUARE = 24.757924
 NUMBER OF TRANSITION USED FOR THE INTEGRAL INVERSION = 29

----- PREDICTED INTENSITIES -----					
ION	SPECTROSCOPIC WAVELENGTH	APPROXIMATE WAVELENGTH	RECONSTRUCTED INTENSITY		Sum[H(i,*)]
			ph/cm2/s	erg/cm2/s	

----- DIFFERENTIAL EMISSION MEASURE -----														
N	TEMP	DEM	N	TEMP	DEM	N	TEMP	DEM	N	TEMP	DEM	N	TEMP	DEM
1	1.00e+04	1.55e+23	11	2.01e+04	1.59e+23	21	4.04e+04	1.20e+23	31	8.11e+04	1.76e+22	41	1.63e+05	2.96e+21
2	1.07e+04	1.56e+23	12	2.15e+04	1.58e+23	22	4.33e+04	1.12e+23	32	8.70e+04	1.38e+22	42	1.75e+05	2.66e+21
3	1.15e+04	1.58e+23	13	2.31e+04	1.56e+23	23	4.64e+04	1.03e+23	33	9.33e+04	1.10e+22	43	1.87e+05	2.42e+21
4	1.23e+04	1.59e+23	14	2.48e+04	1.54e+23	24	4.98e+04	9.29e+22	34	1.00e+05	8.88e+21	44	2.01e+05	2.23e+21
5	1.32e+04	1.60e+23	15	2.66e+04	1.51e+23	25	5.34e+04	8.16e+22	35	1.07e+05	7.29e+21	45	2.15e+05	2.07e+21
6	1.42e+04	1.61e+23	16	2.85e+04	1.48e+23	26	5.72e+04	6.89e+22	36	1.15e+05	6.06e+21	46	2.31e+05	1.95e+21
7	1.52e+04	1.61e+23	17	3.05e+04	1.44e+23	27	6.14e+04	5.49e+22	37	1.23e+05	5.12e+21	47	2.48e+05	1.85e+21
8	1.63e+04	1.61e+23	18	3.27e+04	1.39e+23	28	6.58e+04	4.06e+22	38	1.32e+05	4.38e+21	48	2.66e+05	1.78e+21
9	1.75e+04	1.61e+23	19	3.51e+04	1.34e+23	29	7.05e+04	3.02e+22	39	1.42e+05	3.79e+21	49	2.85e+05	1.73e+21
10	1.87e+04	1.60e+23	20	3.76e+04	1.27e+23	30	7.56e+04	2.29e+22	40	1.52e+05	3.33e+21	50	3.05e+05	1.69e+21
51	3.27e+05	1.68e+21	61	6.58e+05	2.59e+21	71	1.32e+06	7.82e+21	81	2.66e+06	1.74e+21	91	5.34e+06	9.03e+18
52	3.51e+05	1.68e+21	62	7.05e+05	2.83e+21	72	1.42e+06	8.80e+21	82	2.85e+06	1.03e+21	92	5.72e+06	5.32e+18
53	3.76e+05	1.70e+21	63	7.56e+05	3.12e+21	73	1.52e+06	9.87e+21	83	3.05e+06	6.11e+20	93	6.14e+06	3.13e+18

54	4.04e+05	1.73e+21	64	8.11e+05	3.45e+21	74	1.63e+06	1.10e+22	84	3.27e+06	3.62e+20	94	6.58e+06	1.84e+18
55	4.33e+05	1.79e+21	65	8.70e+05	3.85e+21	75	1.75e+06	1.19e+22	85	3.51e+06	2.14e+20	95	7.05e+06	1.08e+18
56	4.64e+05	1.86e+21	66	9.33e+05	4.30e+21	76	1.87e+06	1.20e+22	86	3.76e+06	1.26e+20	96	7.56e+06	6.37e+17
57	4.98e+05	1.95e+21	67	1.00e+06	4.83e+21	77	2.01e+06	1.07e+22	87	4.04e+06	7.47e+19	97	8.11e+06	3.74e+17
58	5.34e+05	2.07e+21	68	1.07e+06	5.44e+21	78	2.15e+06	8.02e+21	88	4.33e+06	4.41e+19	98	8.70e+06	2.20e+17
59	5.72e+05	2.21e+21	69	1.15e+06	6.14e+21	79	2.31e+06	4.94e+21	89	4.64e+06	2.60e+19	99	9.33e+06	1.29e+17
60	6.14e+05	2.38e+21	70	1.23e+06	6.93e+21	80	2.48e+06	2.93e+21	90	4.98e+06	1.53e+19	100	1.00e+07	7.58e+16

---- TEMPERATURE OF MAXIMUM CONTRIBUTION FUNCTION G(T) ----
 ---- AND MEAN TEMPERATURE ----

ION	SPECTROSCOPIC WAVELENGTH	APPROXIMATE WAVELENGTH	TEMPERATURE OF G-MAX	MEAN TEMPERATURE
O + 3	608.3980	0.0000	1.78e+05	1.72e+05
O + 3	787.7110	0.0000	1.78e+05	1.65e+05
O + 3	790.2010	0.0000	1.78e+05	1.64e+05
O + 5	1031.9060	0.0000	2.82e+05	4.90e+05
NE+ 5	469.8290	0.0000	2.00e+05	2.11e+05
NE+ 7	780.3170	0.0000	6.31e+05	9.86e+05
SI+ 2	1206.5050	0.0000	6.31e+04	1.13e+05
SI+ 8	342.9940	0.0000	1.12e+06	1.15e+06
SI+ 8	349.9070	0.0000	1.12e+06	1.15e+06
SI+ 9	347.4270	0.0000	1.41e+06	1.42e+06
SI+10	303.5820	0.0000	1.58e+06	1.79e+06
S + 4	786.4780	0.0000	1.58e+05	1.34e+05
S + 5	933.3750	0.0000	1.78e+05	2.54e+05
S +10	281.4000	0.0000	1.78e+06	1.84e+06
S +10	285.8360	0.0000	1.78e+06	1.84e+06
S +11	288.4500	0.0000	2.00e+06	2.21e+06
CA+ 8	466.2260	0.0000	5.62e+05	6.24e+05
FE+ 8	171.0700	0.0000	8.91e+05	9.78e+05
FE+ 9	345.7220	0.0000	1.12e+06	1.15e+06
FE+ 9	174.5340	0.0000	1.12e+06	1.17e+06
FE+10	352.2500	0.0000	1.26e+06	1.32e+06
FE+ 5	180.4100	0.0000	1.26e+06	1.33e+06
FE+12	348.1830	0.0000	1.58e+06	1.66e+06
FE+12	359.6380	0.0000	1.58e+06	1.66e+06
FE+12	241.3770	0.0000	1.58e+06	1.67e+06
FE+13	211.3150	0.0000	1.78e+06	1.87e+06
FE+14	417.2570	0.0000	2.00e+06	2.16e+06
FE+14	284.1600	0.0000	2.00e+06	2.19e+06
FE+15	360.7420	0.0000	2.24e+06	2.82e+06

References:

[1] A. C. Lanzafame, D. H. Brooks, J. Lang, H. P. Summers, R. J. Thomas and A. M. Thompson, ADAS analysis of the differential emission measure structure of the inner solar corona. Application of the data adaptive smoothing approach to the SERTS-89 active region spectrum., *Astron. Astrophys.*, 384, 242 (2002)

[2] A. C. Lanzafame, D. H. Brooks and J. Lang, ADAS analysis of the differential emission measure structure of the inner solar corona. II. A study of the "quiet Sun" inhomogeneities from SOHO CDS-NIS spectra. *Astron. Astrophys.*, 432, 1063 (2005)

Notes: